scientific reports

Check for updates

OPEN

Adsorption of Bisphenol-A by banana biochar: kinetic, isotherms and thermodynamics

Salah Ud Din[1], Patrick T. Ngueagn[2]✉, Khairia Mohammed Al-Ahmary[3], Hamad AlMohamadi[4], Saedah R. Al-Mhyawi[3], Nuha Y. Elamin[5], Ibtehaj F. Alshdoukhi[6], Jawaher Saud Alrashood[7] & Edwin A. Ofudje[8]

The continuous release of chemical substances like endocrine disruptor bisphenol-A (BPA) can cause harmful health and environmental effects in humans, wildlife and aquatic organisms. This study demonstrates the use of raw and biochar (treated) banana peel adsorbents for the elimination of bisphenol-A in a batch process. The sorption data revealed that optimum adsorption was attained at a pH of 8.0, initial BPA concentration of 240 mg/L, dosage of 0.4 g, and contact time of 200 min and 150 min for raw and treated sample, respectively. From the kinetic study, the pseudo-second-order model (PSOM) best describes treated peels data, indicating chemisorption mechanism, while pseudo-first-order model (PFOM) best explained the kinetic data for the raw sample pointing to physisorption mechanism. The Langmuir model best described the raw banana peel with maximum monolayer adsorption capacities (Q_{max}) of 91.3 mg/g and 135.2 mg/g for the raw and treated sample, while Freundlich model confirmed the adsorption of the BPA by the treated sample to be heterogeneity surface. The thermodynamic characteristics indicate that for the raw banana peel, showed the values of ΔH obtained is 17.42 kJ/mol, while for the treated peel, the value is much higher at 45.01 kJ/mol indicating spontaneous and endothermic process for both adsorbents. These findings highlight the potential of banana peels and its biochar derivative as a sustainable and effective adsorbent in the removal of BPA from wastewater.

Keywords Banana peel, Bisphenol-A, Isotherms, Thermodynamics, Wastewater

Bisphenol-A (BPA) is a chemical substance which is commonly used in the manufacture of resins, plastics, and epoxy resins and it is a known endocrine disruptor and produces harmful health effects in wildlife and humans[1–3]. The wide use of BPA in many consumer products have made it one of the most widely produced chemicals globally, contributing toward an advanced environmental contamination with high potential risk to organisms and human causing severe health problems[1–3]. BPA contaminates water bodies through multiple routes, such as landfill runoff, domestic sewage, and industrial waste, causing disruption of the aquatic ecosystem and persistent contamination[4]. In aquatic organisms, BPA can accumulate leading to behavioural alterations, developmental abnormalities, and reproductive dysfunction[3]. Inhalation, ingestion of contaminated food, and skin contact are the various exposure routes through which BPA can enter the human body[5]. Various health issues in humans, including diabetes, heart disease, breast cancer, obesity, disruption in the endocrine system, and reproductive problems had been linked to prolonged BPA exposure[5,6]. Reduced sperm count, infertility, and symptoms like dizziness, and headaches are the other potential health risks associated with BPA exposure[7]. Due to its persistent and pervasive usage across various industrial applications, the removal of BPA from aqueous

[1]Department of Chemistry, University of Azad Jammu and Kashmir, Muzaffarabad, Pakistan. [2]Department of Inorganic Chemistry, Faculty of Science, University of Yaoundé, 812, Yaoundé, Cameroon. [3]Department of Chemistry, College of Science, University of Jeddah, Jeddah, Saudi Arabia. [4]Department of Chemical Engineering, Faculty of Engineering, Islamic University of Madinah, Madinah, Saudi Arabia. [5]Department of Chemistry, College of Science, Imam Mohammad Ibn Saud Islamic University (IMSIU), P.O. Box 5701, 11623 Riyadh, Saudi Arabia. [6]Department of Basic Sciences, College of Science and Health Professions, King Saud bin Abdulaziz University for Health Science, King Abdullah International Medical Research Center, Riyadh, Saudi Arabia. [7]Department of Teaching and Learning, College of Education and Human Development, Princess Nourah bint Abdulrahman University, Riyadh, Saudi Arabia. [8]Department of Chemical Sciences, Mountain Top University, Ibafo, Ogun State, Nigeria. ✉email: patrickngueagn@gmail.com

solutions has emerged as an important area of concern among researchers[8]. This has necessitated the exploration of effective methods for its remediation so as to mitigate its potential health and ecological impacts.

Various conventional methods have been engaged in the remediation of BPA from contaminated water, and these include the likes of chemical precipitation, ion exchange, ozonation, adsorption, membrane filtration, and electrochemical treatment[9,10]. While these methods offer several advantages, their wide usage has been hampered due to their secondary waste generation, high operational costs, and inability to completely remove wide spectrum of contaminants[10]. Adsorption remains one of the most versatile and effective techniques for the removal of water contaminants due to its operational simplicity, minimal sludge generation, cost-effectiveness, and adaptability to treat a wide variety of contaminants[11]. Compared with membrane separation, advanced oxidation, or chemical precipitation, adsorption requires relatively low energy input, can be carried out under mild conditions, and often employs materials that can be reuse that support large scale application which makes it affordable technique for pollutants removal in wastewater treatment contexts[12]. Tiliouine et al.[13]. observed that simple agricultural biosorbents such as powdered myrtle leaves have shown to deliver competitive adsorption performance for dyes, underscoring the potential of locally available and low-cost biomass as effective adsorbents. Moreover, valorization of agro-food residues via hydrothermal carbonization provides a sustainable means to tailor adsorbent surface chemistry and porosity while supporting circular economy objectives[14]. With the raising cost of activated carbon production being the most widely used adsorbent, agricultural wastes have been considered as high and promising effective adsorbent for BPA removal from wastewater[15].

Biochar, a carbonaceous material which is also eco-friendly is a promising potential adsorbent for removing different inorganic and organic pollutants from the environment[16]. These biomass-derived materials are very effective in various contaminants removal due to their availability in diverse functional groups and high surface area[17]. Bananas are the fourth most cultivated fruits worldwide, however their peels are often discarded causing environmental pollution[18]. The main composition of banana peels are hemicellulose (25.52%), cellulose (11.45%), and lignin (9.82%)[19]. With this rich composition, banana peels is thus a promising source of biochar production. In addition, with the presence of functional groups like hydroxyl, aromatic rings, carboxyl, amino, and alkyl groups, banana peel biochar could significantly bind to endocrine-disrupting contaminant like BPA[20]. Thus, these peels, which are often discarded as agricultural waste, can be converted into biochar, serving as an eco-friendly solution in wastewater treatment[21–23]. Since Bisphenol-A is a persistent endocrine-disrupting compound with well-documented adverse effects on human health, yet its effective and affordable removal from wastewater remains challenging. Although banana peels are an abundant agro-waste generated globally, their valorisation into biochar for targeted BPA adsorption has received little attention. This study uniquely addresses this gap by converting discarded banana peels into a sustainable, low-cost adsorbent and directly comparing its performance with untreated peel, providing a waste-to-resource solution that mitigates a pollutant of high environmental and public-health concern.

Materials and methods

Biochar preparation and characterizations

Banana peels (BP) were collected, washed thoroughly with deionized water, and sun dried for 72 h. The dried peels were then pyrolyzed under an inert nitrogen atmosphere at 600 °C for 2 h in a muffle furnace. The pyrolysis process was carried out in a muffle furnace with a controlled heating rate of 5 °C/min until the target carbonization temperature of 600 °C was reached, followed by holding for 1 h. To ensure an inert atmosphere during carbonization, the furnace chamber was continuously purged with high-purity nitrogen gas (≥ 99.9%) at a flow rate of 3 mL/min throughout the process, starting 10 min before heating and maintained until the furnace cooled to below 100 °C.The resulting biochar was cooled, washed to remove residual ash or impurities, ground, and sieved to obtain a uniform particle size. The biochar obtained from the banana peel (treated) and the uncalcined banana peel (raw) were stored in an airtight container. The prepared biochar was examined with various analytical techniques like Fourier Transform Infrared Spectroscopy (FT-IR) (CARY630 NBY, Thermo Fisher Scientific Instrument, Waltham, MA, USA) for the identification of various functional groups responsible for the dye adsorption. Scanning Electron Microscopy (SEM) (Phenom ProX, USA) was used to observe surface morphology and porosity of the adsorbent. Brunauer-Emmett-Teller (BET) Analysis was utilized to determine surface area and pore size distribution (Quantachrome NOVA 2200 C, USA). The point of zero charge (pH_pzc) of the raw banana peel and banana peel biochar was done using the pH-drift method with 0.01 M NaCl as the background electrolyte. Different aliquots of the NaCl solution were made and 50 mL of this was placed in 100 mL conical flasks, and the initial pH values were adjusted from 2.0 to 8.0 using 0.1 HCl or NaOH. The initial pH (pH_0) of each solution was recorded. Thereafter, 0.05 g of the adsorbent was added to the 50 mL solution and the flasks were agitated on an orbital shaker at 150 rpm for 12 h at room temperature. After this, the suspensions were allowed to settle, and the final pH (pH_f) was determined. The difference between final and initial pH ($\Delta pH = pH_f - pH_0$) was evaluated for each sample, and ΔpH was plotted against pH_0. The pH_pzc was identified as the point at which ΔpH equals zero. Thermogravimetric behaviour of the adsorbent was assessed using TGA 4000, Perkin Elmer, Haarlem, (Netherlands).

Preparation of Bisphenol-A solution and adsorption study

Bisphenol-A stock solution of 1000 mg/L was made by dissolving analytical-grade of Bisphenol-A in deionized water. Working solutions of different concentrations were made by appropriate dilution and the solution pH was adjusted using 0.1 M HCl or NaOH before sorption studies. Thereafter, 0.4 g dose of biochar was reacted with 20 mL of Bisphenol-A solution in conical flasks. The mixture was shaken at a constant temperature (45 °C) for a predetermined time. After adsorption, the samples were filtered, and the residual Bisphenol-A concentration was investigated with the use of UV-Vis spectrophotometer (Shimadzu UV-3600 UV-Vis-NIR) at a wavelength of 280 nm. The effects of initial concentration, pH, contact time, biochar dosage, and temperature, were

systematically evaluated following same procedure. The experiments were performed in triplicate for each batch condition to ensure reproducibility and the average value was documented. The amount adsorbed (q_e, mg/g) and the percentage removal (%) were obtained from Eqs. 1 and 2:

$$q_e = \frac{C_o - C_e}{m} \times V \tag{1}$$

$$R(\%) = \frac{C_o - C_e}{C_o} \times 100 \tag{2}$$

Where C_o, C_e, v and m denote the initial BPA concentration (mg/L), BPA concentration at equilibrium (mg/L), volume (L) of BPA used and mass (g) of the biochar.

Desorption study

Desorption experiments were conducted using EDTA to assess the reusability of biochar. The regenerated biochar was reused for multiple adsorption-desorption cycles to evaluate its long-term efficiency. The percentage of Bisphenol-A recovery was determined to assess the feasibility of biochar for practical applications. The percentage desorption was computed using Eq. 3:

$$\%D = \frac{AD}{AA} X100 \tag{3}$$

Where D denotes the desorption, AA stands for the amount adsorbed, and AD represents the amount desorbed.

Results and discussions

FT-IR analysis

The FT-IR spectra which compare banana biochar before (a) and after (b) the adsorption of Bisphenol-A is shown in Fig. 1. Spectrum a, illustrates the surface characteristics of biochar which shows a weak band around 3465 cm^{-1}, that corresponds to O–H stretching vibrations often associated with hydroxyl group from alcohols or moisture[24–26]. The region around 1745, 1680 and 1445 cm^{-1} shows features possibly associated with C = O,

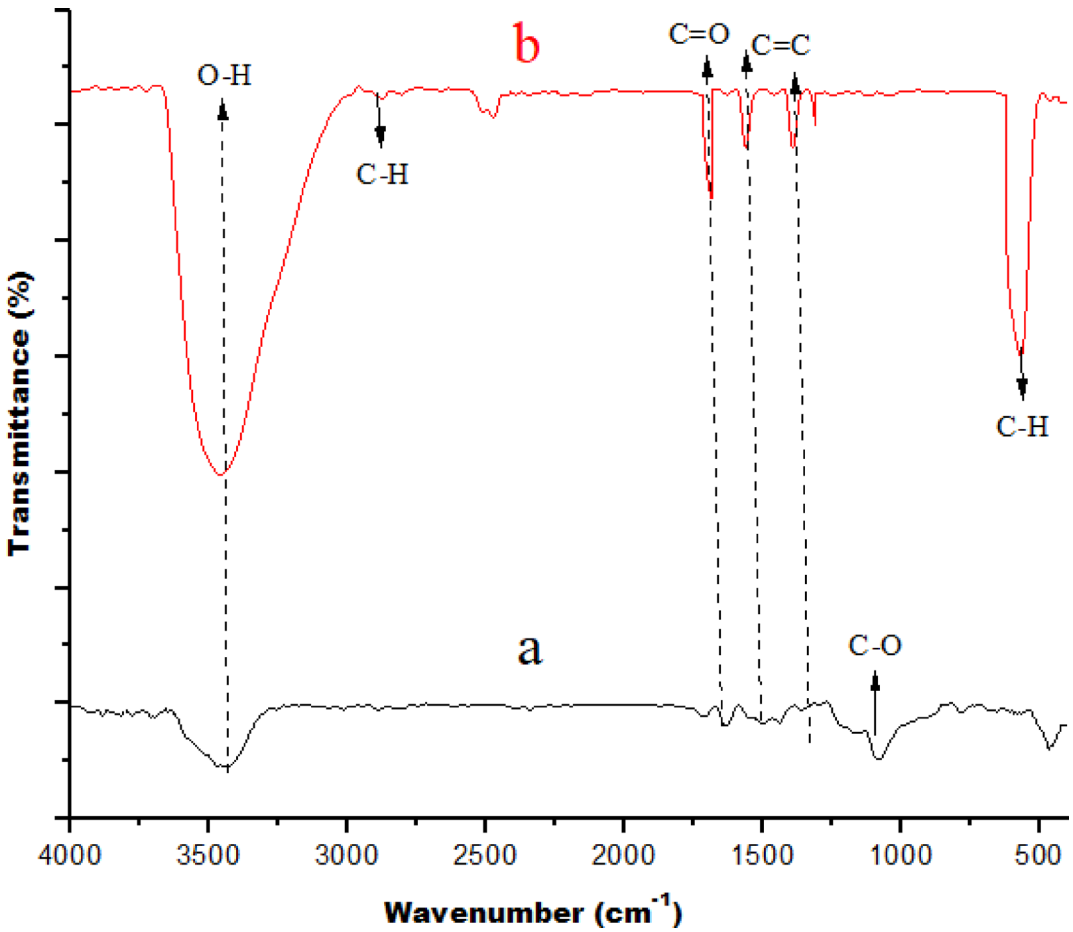

Fig. 1. FT-IR investigation of banana biochar before (a) and after BPA adsorption (b).

and C = C stretching[24], while the peak which corresponds to C–O is seen at 1260, 1105 and 1030 cm^{-1}[25,26]. Below 1000 cm^{-1}, the spectrum shows minor peaks that may be bending or inorganic components such as Si–O. In contrast, spectrum b, taken after BPA adsorption, displays several notable changes. A strong and broad absorption band appears around 3455 cm^{-1} due to O–H stretching indicating the involvement of this group in the adsorption process suggesting involvement in hydrogen bonding with BPA's hydroxyl groups. Additionally, sharp peaks emerge in the range of 1650–1584 cm^{-1} regions, which are characteristic of aromatic C = C stretching vibrations or reduced C = O peaks. This suggests strong π–π interactions between the aromatic rings of BPA and the conjugated domains within the carbonaceous biochar matrix as these π–π stacking interactions are common in adsorption of aromatic pollutants onto graphitic surfaces. The peaks initially seen in the region between 1260 1105, and 1030 cm^{-1} completely disappeared which suggests the likely involvement of C-O bonds in the adsorption process, implying direct interactions with the likes of hydrogen bonding between BPA and these oxygen-containing groups. Notably, the sharp features below 600 cm^{-1} may be related to aromatic ring deformation and additional C–H bending vibrations. These spectral changes clearly indicate that BPA molecules successfully interacted with the banana biochar surface functional groups. These interaction mechanisms (π–π stacking and hydrogen bonding) have been widely reported in recent literature as governing the adsorption of aromatic pollutants like BPA on biochar[27–29]. These findings support a dual mechanism where both physical interactions (physisorption) and specific functional group associations (chemisorption) contribute to BPA uptake, consistent with the kinetic and thermodynamic data discussed in later sections.

SEM analysis biochar adsorbent

The surface morphology of the biochar before adsorption is shown in SEM image labeled a (Fig. 2). The presence of small particle sizes with porous network can be seen in the structure. There are visible cavities and voids distributed within the surface, indicating a well developed porous texture that is suitable for adsorption process. These pores network plays a critical role in the sorption of pollutants like BPA since it offers a high surface area. The SEM image labeled as b which illustrates biochar after BPA adsorption appears more compact and smoother, in which many of the visible pores previously seen are partially or completely filled. The biochar particles appears more aggregated, and a sizeable reduction in the size and number of open voids was noticed. This indicates that BPA molecules were successfully adsorbed onto the the adsorbent surface and most likely into the internal pores of the biochar adsorbent.

Pore properties analysis

The graph which was used to evaluate the porous characteristics of the biochar material is shown in Fig. 3. The cumulative pore volume curve represents the total pore size accumulated as the pore diameter rises (Fig. 3a). It was observed in the graph that the cumulative pore volume rose steadily from 1.83 nm to 2.82 nm, indicating a substantial number of mesopores (pores between 2 and 50 nm). The upward trend suggests a broad distribution of pore sizes which implies that the biochar has a well-developed porous structure, suitable for adsorption process as can easily allows BPA molecules to interact and diffuse with internal surfaces. The data presented in Fig. 3b depicts BET adsorption isotherm graph which provides the surface area and adsorption behavior of adsorbents. The surface area of 84.21 m^2/g and 114.25 m^2/g for raw and biochar banana samples respectively with the biochar material demonstrating higher BET surface area which could enhance the adsorption potency of adsorbent. The treatment seems to have improves the surface are, and enhanced the porosity substantially.

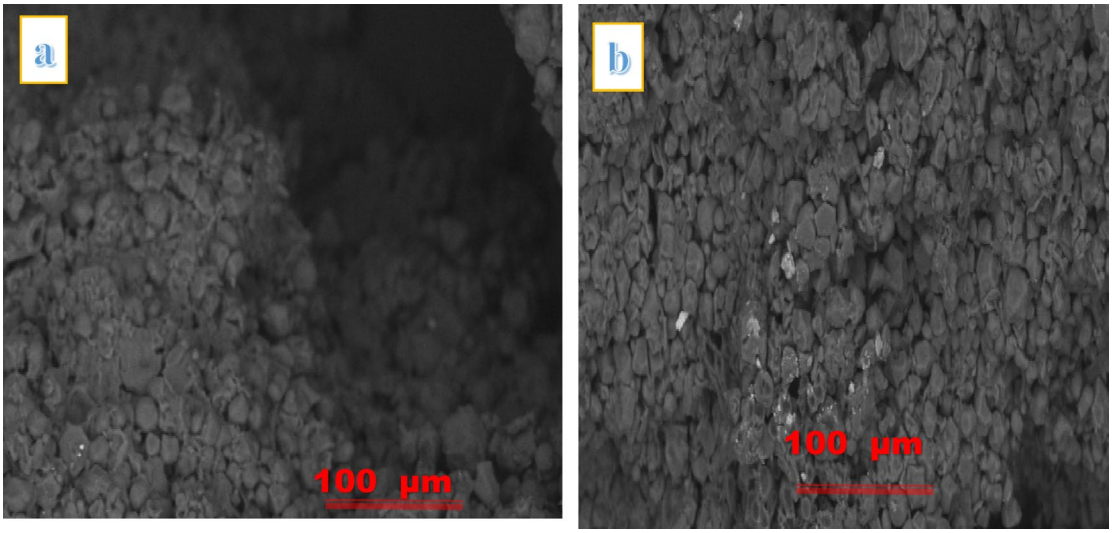

Fig. 2. SEM investigation of banana biochar before (a) and after BPA adsorption (b).

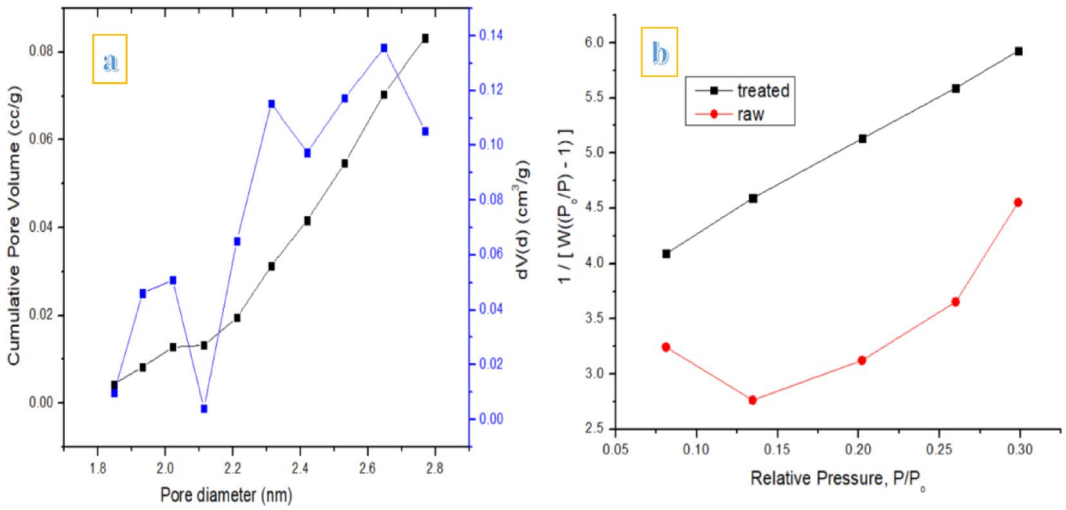

Fig. 3. Pore size (a) and BET (b) of investigation of banana peel.

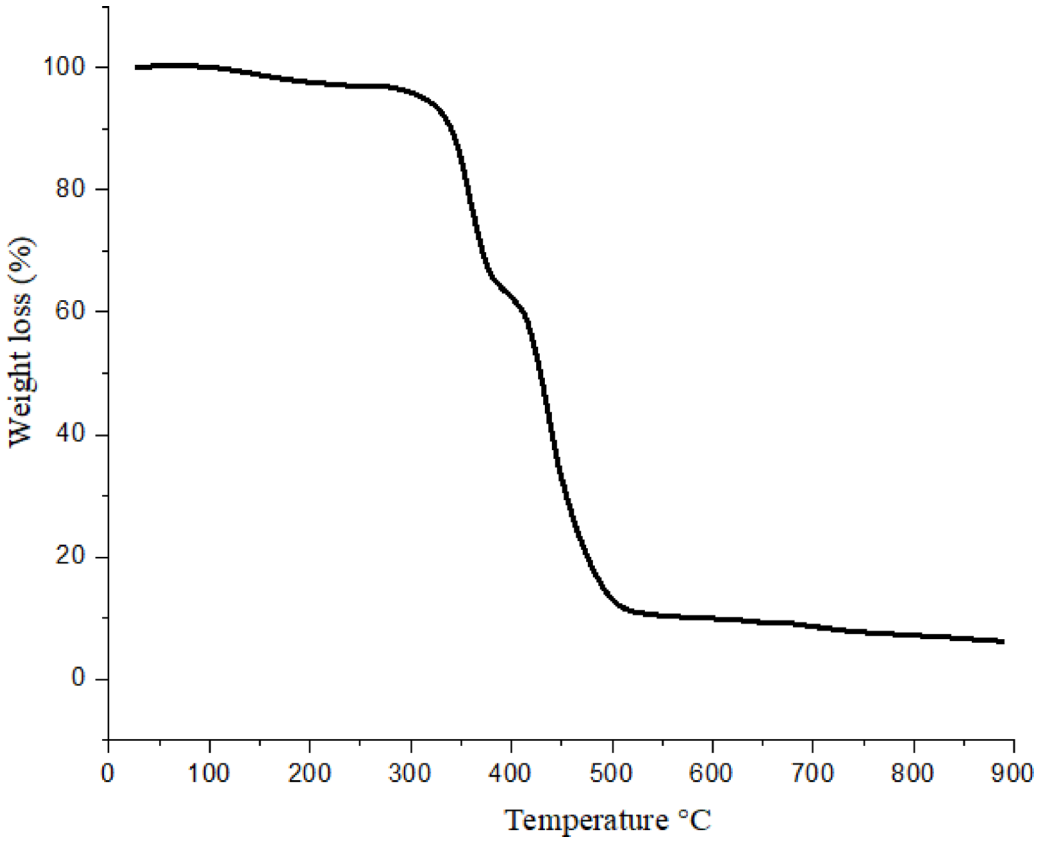

Fig. 4. TGA investigation of banana peel adsorbent.

Thermogravimetric study

The thermogravimetric analysis (TGA) graph shows the thermal profile of banana peel as illustrated in Fig. 4. In the beginning (below 150 °C), a slight loss in weight was observed and this is attributed to the evaporation of moisture from the surface and most likely any physically adsorbed water[30,31]. The second and most prominent stage of weight loss was observed between 200 °C and 470 °C and this phase depicts the thermal decomposition of the of banana peel's major organic components, which includes the likes of cellulose and hemicellulose[30,31]. This reduction in mass shows the volatilization of organic matter of the banana peel's and its conversion into carbonaceous materials. Between 480 and 600 °C, the final stage of weight loss was noticed and this degradation illustrates the breakdown of lignin and the likely transformation of remaining organic matter into stable

carbonaceous residues[30,31]. Above 600 °C, the graph becomes flat, indicating the formation of thermally stable ash.

Effect of contact time and BPA concentration

The adsorption of Bisphenol-A by raw and treated banana peels, as shown in Fig. 5, is influenced greatly by both contact time and the initial dye concentration. The amount of dye adsorbed increased steadily with contact time, especially in the early stages of the process. At a concentration of 240 mg/L, the adsorption of BPA by the raw material (Fig. 5a) surged from 19.4 mg/g to 87.9 mg/g by 200 min, where it becomes constant even up to 300 min. In the case of the treated sample, the adsorption capacity rose from 30.3 mg/g at 10 min to 131.5 mg/g by 150 min and thereafter remains constant. The aggressive uptake seen at the beginning indicates that the majority of the dye is adsorbed because of the high availability of active sorption sites on the biochar surface[32]. But as the reaction progresses with time, the system approaches equilibrium as these sites become increasingly occupied and beyond this point, no significant uptake is observed, and this reflects the maximum adsorption capacity of the adsorbent was attained at 200 min and 150 min for raw and treated sample respectively. In addition, biochar gets to equilibrium faster than raw banana and this indicates that biochar achieves faster kinetics in addition to higher capacity, making it more effective for water treatment. Supong et al.[28]. observed while using activated carbon obtained from *Tithonia diversifolia* biomass that a maximum 98.2% removal percentage was achieved at optimum contact time of 80 min and dye concentration of 40 mg/L. In a study conducted by Rahmat et al.[33]., it was observed that both the adsorption capacity and percentage removal of BPA rose parallel with the contact time with optimum percentage removal of 59.97% achieved at 4 h and this was attributed to available external sites at the initial stage of the reaction.

Initial dye concentration is another major factor that influences adsorption capacity. The data from the study on the role of initial concentration of Bisphenol-A clearly demonstrates that the amount of dye adsorbed by both raw and treated banana peel increases as dye concentration. In the case of the raw data and at 100 min of contact time, the adsorption capacities surged from 13.4 mg/g for 40 mg/L, to 76.3 mg/g for 240 mg/L.

For the treated sample however (Fig. 5b), the data reveals that at 150 min contact time, the sorption rose from 23.4 mg/g at 40 mg/L to 131.5 mg/g at 240 mg/L. This trend is attributed to a greater concentration gradient, could acts as a driving force, enabling the mass transfer of more dye molecules from the aqueous phase to the surface of the adsorbent. Even at lower dye concentrations (80 mg/L and 100 min), biochar outperforms raw banana by achieving adsorption of 39.5 mg/g, when compared with 28.3 mg/g for the raw sample which could be attributed to enhanced surface area, pore volume, and possibly improved functional groups provided by the biochar giving rise to more binding sites and stronger interactions with dye molecules. This substantial difference indicates how the pyrolysis process improved the adsorption properties of the biochar material by creating more sorption sites, thus making it more effective for dye removal. Mat et al.[24]. investigated agricultural wastes, including coconut bunch and banana bunch for BPA adsorption and they noted that the highest removal of BPA was obtained when the concentration was raised from 5 to 100 mg/L, and they attributed this to the higher chances of collision between particles of the adsorbents and molecules of BPA caused by the driving force which was greater at the beginning and that higher concentration helps to overcome all mass transfer resistances between BPA molecules and adsorbents.

Effects of pH

The action of pH on the uptake of Bisphenol-A by both raw and banana biochar plays an essential role in determining adsorption efficiency. The behaiour of BPA under different values can also be explained using the information derived from point of zero charge (pH_pzc). The results reveal that the pH_pzc was 4.65 for the raw peel and 4.24 for the biochar Fig. 6a. Since BPA has a pK_a of approximately 9.6, it exists predominantly in its

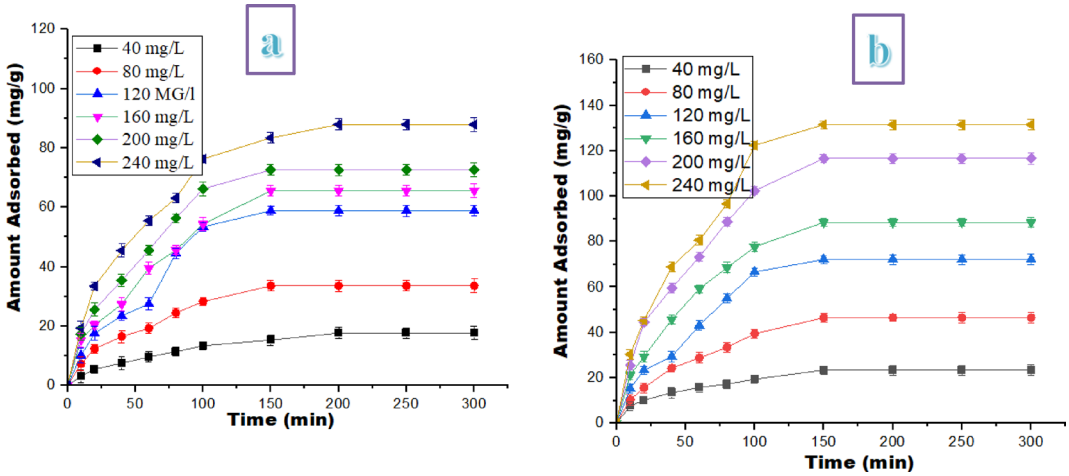

Fig. 5. Contact time and BPA concentration impact on the adsorption capacity of raw (a) and treated banana peel adsorbents (b).

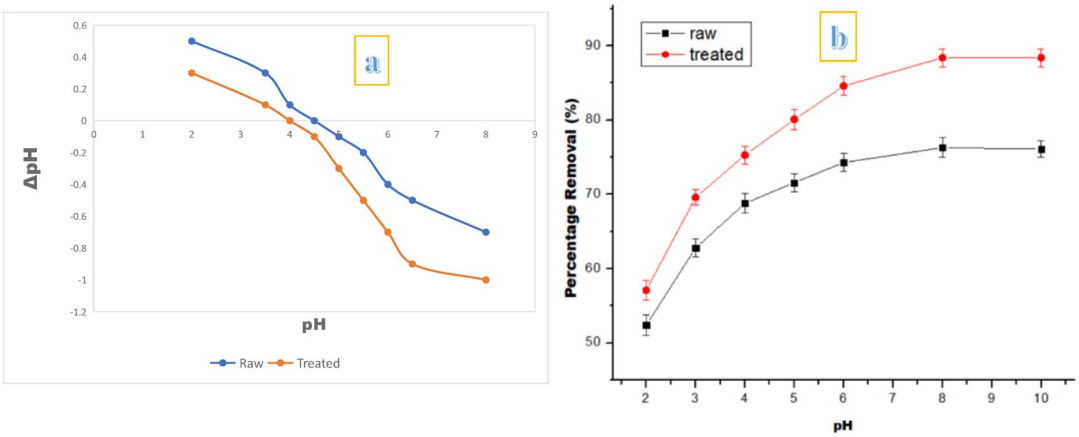

Fig. 6. Point of zero charge (pH_pzc) (a) and pH impact (b) on the adsorption capacity of raw and treated banana peel adsorbents towards BPA uptake.

neutral molecular form under our experimental pH range (4–8)[34]. This imply that at solution pH values greater than the pH_pzc, the adsorbent surface becomes negatively charged, which can improve adsorption through hydrophobic interactions and π–π electron donor–acceptor interactions rather than electrostatic attraction (since BPA is neutral at these pH values)[35]. At pH values below pH_pzc, the surface is positively charged, but since BPA is still neutral, the adsorption is mainly governed by π–π interactions and hydrogen bonding rather than charge–charge forces. The observed higher adsorption efficiency near neutral to slightly acidic pH aligns with these mechanistic considerations[36]. The data shown in Fig. 6b indicate a clear relationship between adsorption capacity of the adsorbent and the solution pH of the dye, with clear differences between the two adsorbents. For the raw banana peel, the uptake capacity rose gradually with pH from 52.4% at pH 2 to a maximum of 76.3% at pH 8 and the a slight decline at pH 10 (76.1%), but this change is small, suggesting near-optimal adsorption occurs at neutral to slightly basic pH. In the case of the biochar, the adsorption is higher with values increasing from 57.1% at pH 2 to 88.4% at pH 8, and remains almost constant at pH 10.

The rise in adsorption efficiency with pH can be explained from the ionization behavior of Bisphenol-A, which is a weakly acidic molecule with a pKa of around 9.6. At acidic conditions (low pH), BPA exists primarily in its non-ionized (neutral) form, and the banana surface, contains likely positively charged functional groups as a result of protonation, which could cause less interaction or repel these molecules. This could explain the low uptake seen within this pH range. But as the pH rises, the Bisphenol-A molecules starts to ionize into its anionic causing the surface to becomes less positively charged, and the interactions between the pollutant molecules and the positively charged surface of the banana adsorbent become stronger due to the available active sites on the adsorbent surface through electrostatic attraction or hydrogen bonding[37]. The results of this study is consistence with the findings of Wirasnita et al.[38]. where is was reported that the maximum uptake capacity of BPA by empty fruit bunch activated carbon was achieved over the entire pH range of 2 to 9. But on the contrary, Wang and Zhang[27] observed that maximum adsorption capacity of magnetic biochar to bisphenol-A took place at pH of 3 and this was attributed to the formation of π–π electron donor–acceptor interaction that occurred between the bisphenol-A molecules and magnetic biochar surface, accompanied by a strong H-bond.

Effect of adsorbent dosage

The effect of adsorbent dosage on the uptake of BPA by raw and biochar from banana peel are provided in Fig. 7 which reveals that as the dosage increases, both materials exhibit an initial improvement in dye uptake, but the trend eventually declines slightly at higher dosage. In the case of the raw banana peel (Fig. 7a), the sorption percentage of BPA increases with adsorbent dosage from 55.3% at 0.1 g to 77.4% at 0.4 g. and above this point, there is a slight decline in sorption to 75.6% at 0.5 g and 74.5% at 0.6 g. For the biochar (Fig. 7b), the trend is similar but with higher adsorption values as the sorption rose from 61.4% at 0.1 g to a maximum of 87.1% at 0.4 g, and thereafter slightly reduced to 86.3% at 0.5 g and 86.1% at 0.6 g.

The larger surface area and greater number of available active sites provided by the increased mass of material may have caused initial increase in adsorption observed[27,39]. But with more adsorbent and constant adsorbate volume, there are less binding chances for dye molecules in the solution due to particle agglomeration and site overlapping leading to reduced uptake. With too much adsorbent, clustering of the particles may reduce the effective surface area there by leading to a decrease in the number of available adsorption sites[27,39]. In contrast, the amount of BPA adsorbed per unit mass of adsorbent (q_e) showed a continuous decline with increasing dosage in both figures, dropping from about 48.9 mg/g to 23.5 mg/g in Figure a, and from 58.2 mg/g to about 44.1 mg/g in Figure b. This inverse relationship between dosage and q_e is attributed to the fixed initial BPA concentration being distributed over a larger mass of adsorbent at higher dosages, leading to unsaturated active sites and reduced adsorption capacity per gram.

The reasons for the better efficiency for the biochar as against the raw material could be due to the biochar's higher porosity, and larger surface area resulting from the carbonization process which enhanced it to adsorb more of the dye molecules even as dosage increases. The study carried out by Wang and Zhang[27] demonstrated

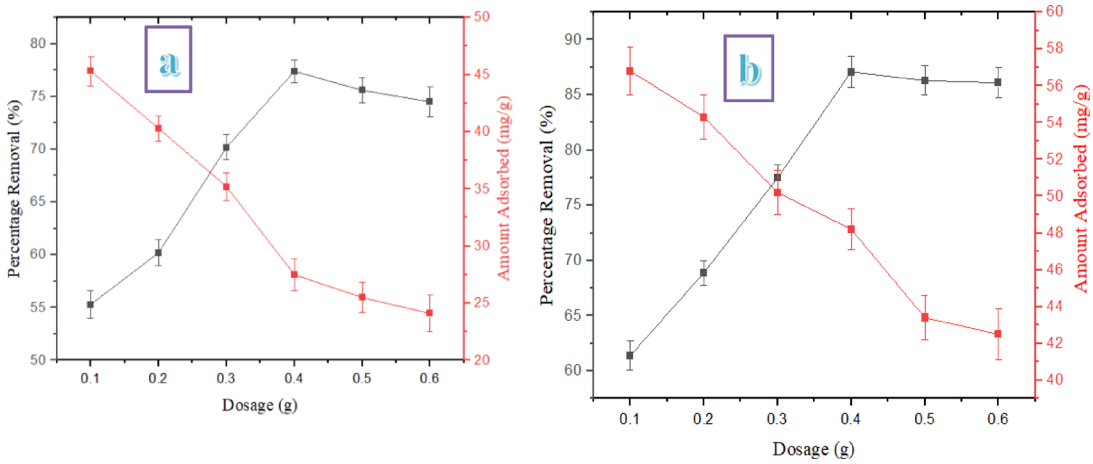

Fig. 7. Raw (a) and treated (b) banana peel adsorbents impact on the adsorption capacity of BPA.

		Raw						Treated					
	C_o(mg/L)	40.00	80.00	120.00	160.00	200.00	240.00	40.00	80.00	120.00	160.00	200.00	240.00
First order	Q_e (exp) (mg/g)	17.7	33.6	58.8	65.6	72.6	87.9	23.4	46.5	72.2	88.4	116.6	131.5
	Q_e (cal) (mg/g)	16.7	34.02	57.3	64.2	73.3	87.2	26.5	41.4	68.3	84.1	96.1	121.4
	k_1(mins^{-1})	0.043	0.051	0.083	0.114	0.127	0.142	0.103	0.115	0.131	0.157	0.182	0.201
	R^2	0.994	0.993	0.994	0.978	0.986	0.996	0.853	0.726	0.806	0.866	0.870	0.910
	% SSE	0.014	0.012	0.011	0.015	0.007	0.005	0.103	0.124	0.148	0.065	0.132	0.048
Second order	Q_e (cal) (mg/g)	13.1	25.6	46.7	50.5	68.3	78.1	22.5	43.4	73.8	89.2	114.8	129.1
	k_2 (g/mg/min)	0.112	0.122	0.146	0.168	0.183	0.202	0.162	0.193	0.204	0.255	0.342	0.542
	R^2	0.897	0.92	0.89	0.93	0.91	0.93	0.99	0.98	0.97	0.98	0.97	0.99
	% SSE	0.014	0.382	0.255	0.342	0.093	0.423	0.014	0.025	0.006	0.003	0.008	0.013
Intra particle diffusion	K_p (mg/g/mins$^{1/2}$)	2.413	2.938	3.504	3.839	5.824	9.318	3.191	5.802	7.224	10.715	14.306	17.421
	Ci (mg/g)	0.429	0.825	1.504	1.806	2.118	3.702	0.638	0.863	1.725	3.308	5.801	6.903
	R^2	0.96	0.95	0.92	0.94	0.92	0.94	0.91	0.97	0.99	0.98	0.95	0.99

Table 1. Kinetic model constants for Bisphenol-A removal using Raw and Biochar banana Peel adsorbents.

a significant increase in BPA removal efficiency (up to ~80%) as the adsorbent dosage of magnetic biochar rose, but, that the saturation of the adsorbent surface led to marginal gains beyond a specific dosage which caused reduced uptake due to particle agglomeration or site overlap. According to Shao et al.[39], increasing biochar adsorbent dosage led to a larger surface area for adsorption process and this eventually resulted in better effectiveness in removing contaminant.

Adsorption kinetics models

Pseudo-first-order kinetics

The PFOM assumed that adsorption occurs through weak van der Waals forces and that the number of available sites of adsorption determines the bind of the pollutant to the adsorbent surface. Mathematically, the linear representation of this model is shown in Eq. 4, while the sum of squared errors (%SSE) used for verifying the acceptability of the best model is given in Eq. 5 below[27,37,40]:

$$\log(Q_e - Q_t) = \log Q_e - {}^{k_1}/_{2.303}t \tag{4}$$

Here, k_1 is the rate constant from the pseudo-first-order (min^{-1}), and t is time (min), while Q_t and Q_e have been defined previously.

$$RMSE = \sqrt{\frac{\sum_{i}^{N}(Q_{(\exp)} - Q_{(cal)})^2}{N}} \tag{5}$$

N expresses the data points number, while the remaining parameters have been defined previously. The parameters presented in Table 1 were deduced using Fig. 8a. For this model, the values of the adsorption capacities as obtained from the experimental equilibrium data (Q_e,exp) increase with dye concentration for both

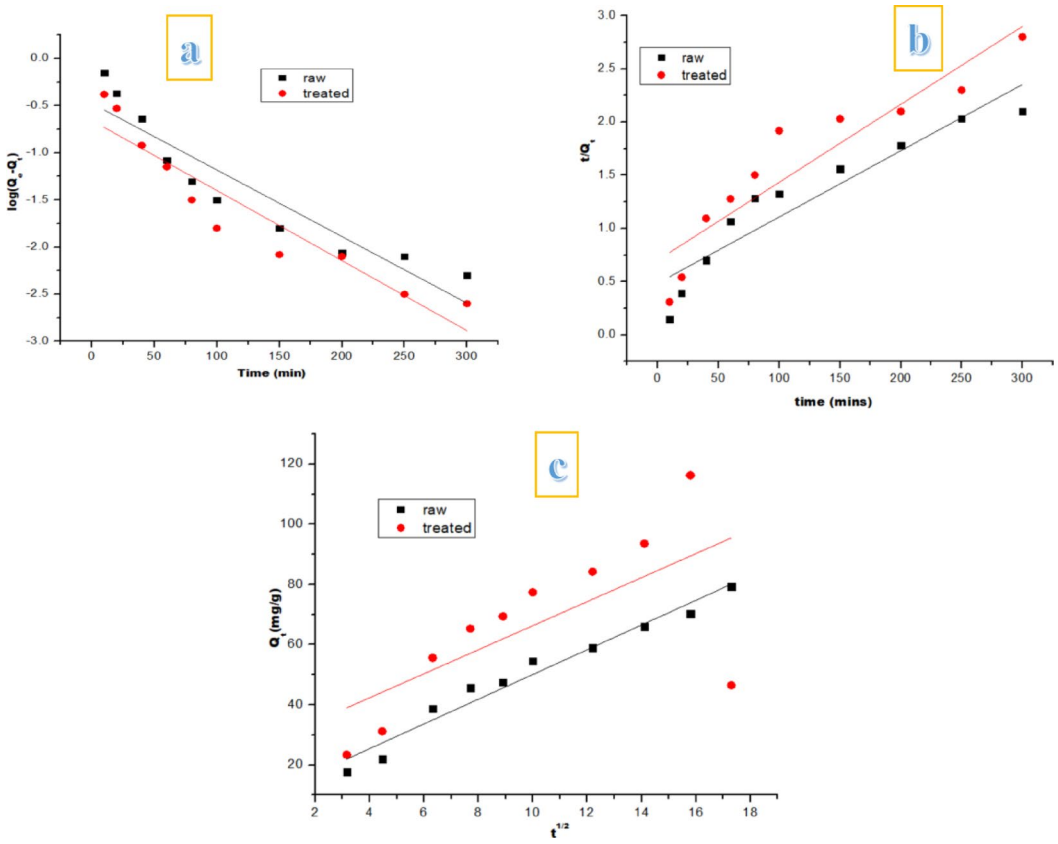

Fig. 8. Kinetic plots of (a) PFOM, (b) PSOM, and (c) Intraparticle diffusion toward the sorption of BPA by raw and treated banana peel.

raw and treated banana peels, though the sample from the treated peels demonstrated higher capacities across all concentrations. The calculated adsorption capacities (Q_e,cal) are close to the experimental values for the raw samples, while the coefficients of determination values (R^2) are very high (above 0.97) for the raw samples as well, indicating a good fit of the model. This is supported from the low values of sum of squared errors (%SSE) observed. However, for treated peel samples, R^2 values drop, the sum of squared errors (%SSE) values increases with wide range of gaps between the values of the calculated adsorption capacities and the experimental values. These trends indicate that while the pseudo-first-order model is reasonably suitable to describe adsorption kinetics behaviour of the raw banana peel to be physisorption mechanism, it is not well-suited for predicting the treated peels.

Pseudo-second-order kinetics

The PSOM model assumed that adsorption takes place via stronger chemical forces, and mathematically, the linear representation of this model is shown in Eq. 6 below[27,37,40]:

$$t/Q_t = 1/k_2 Q_t + t/Q_e \tag{6}$$

Here, k_2 is the rate constant from the pseudo-second-order (g/mg·min), while Q_t and Q_e have been defined previously. The parameters presented in Table 1 were deduced using Fig. 8b. In contrast to what what was observed for the PFOM, the PSOM gave a much better fit for the treated banana peel. The experimental Q_e values are very close to the calculated ones, with the values of R^2 consistently higher (≥ 0.97), suggesting a strong correlation and indicating that chemisorption is most likely the dominant mechanism in the adsorption process. This was corroborated by the low values of the %SSE, ranging from 0.003 to 0.025, thus, confirming the model's accuracy in describing the adsorption process. For the raw banana peel, this model still fits partially though with lower R^2 values (around 0.89 to 0.93) and higher SSE values at certain concentrations.

Intraparticle diffusion model

Intraparticle diffusion refers to the transport of molecules within the pores of a solid material, and mathematically, the linear representation of this model is shown in Eq. 7 below[27,37,40]:

$$Q_t = k_P t^{1/2} + C_i \tag{7}$$

Here, k_p denotes rate constant for intra-particle diffusion (mg/g/min$^{1/2}$), whereas C_i stands for boundary layer thickness. The parameters listed in Table 1 were obtained using Fig. 8c. The diffusion rate constants (k_p) values rose with initial dye concentration with the treated peels having higher values, reflecting improved pore structure and most likely, diffusion pathways because of the biochar treatment. The intercepts (C_i) are also higher for treated peels than the raw samples, suggesting more prominent boundary layer effects and suggesting that surface adsorption plays a substantial role. The values of R^2 are high for both samples (up to 0.99), but the non-zero intercepts suggests that intraparticle diffusion may not be the sole rate-limiting step in the process. The process can be described in three different stages. First, is the external mass transfer also known as film diffusion, where the dye molecules move from the bulk solution to the outer surface of the adsorbent's particle; second is the intraparticle or pore diffusion, in which the dye molecules penetrate and diffuse via the internal pores of the adsorbent and this step can be rate-limiting[27,37]. Stage three is the adsorption, where the dye molecules react with active binding sites on the adsorbent's internal or external surfaces.

Isotherms studies

Langmuir isotherm

The Langmuir isotherm describes the adsorption of molecules onto the surface of solids, and assumed that adsorbed molecules do not interact with each other with a monolayer coverage where all adsorption sites are equivalent. Mathematically, the linear representation of this model is shown in Eq. 8, while the expression for the separation factor from the Langmuir model, (R_L) is depicted in Eq. 9 below[37,40]:

$$C_e/Q_e = 1/bq_m + C_e/Q_m \tag{8}$$

Here, Q_{max} stands the maximum adsorption capacity (mg/g), b is the Langmuir constant (L/mg), while C_e (mg/L), and Q_e (mg/g) have both been defined previously.

$$R_L = 1/(1 + bC_o) \tag{9}$$

Using the linear regression method, the data obtained from Fig. 9a are presented in Table 2. The obtained maximum monolayer adsorption capacity (Q_{max}) showed that the treated banana peel had higher value (135.2 mg/g) when compared with the raw peel (91.3 mg/g), inferring that biochar treatment greatly enhances the capacity of the adsorbent. This might likely due to improved porosity, surface area, and chemical reactivity from the biochar structure. Values from R_L analysis shows that they are between 0 and 1, thus depicting the favorability of the adsorption process[37,40] with the treated peel samples having lower values of 0.25 when compared with the raw peel (0.63). This indicates that the sorption of BPA onto treated banana peel is more

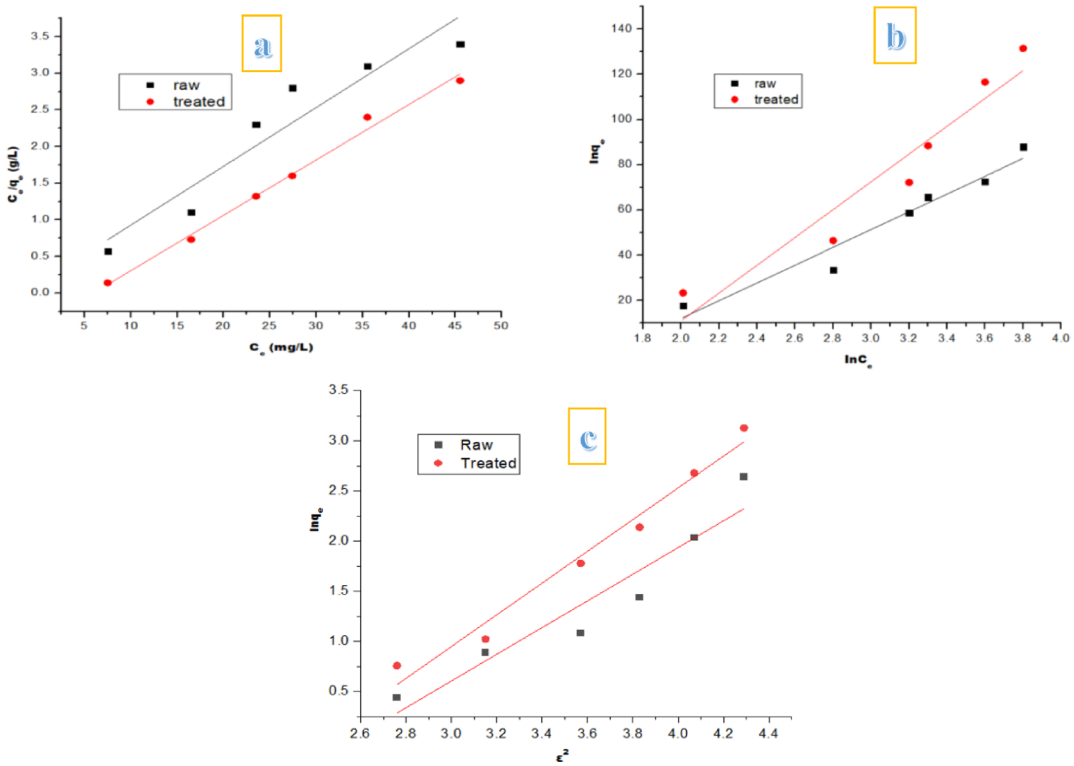

Fig. 9. Isotherm models of (a) Langmuir, (b) Freundlich, and (c) Dubinin-Radushkevich toward the adsorption of BPA by raw and treated banana peel.

	Parameters	Raw banana peel	Treatedbanana peel
Langmuir	Q_{max} (mg/g)	91.3	135.2
	R_L	0.63	0.25
	R^2	0.93	0.99
Freundlich	K_F (mg/g)(L/mg)$^{-1/n}$	45.51	66.12
	1/*n*	0.50	0.27
	R^2	0.95	0.97
Dubinin–Radushkevich	Qs (mg/g)	58.28	77.24
	E (kJ/mol)	5.61	16.19
	R^2	0.94	0.97

Table 2. Isotherm model constants for Bisphenol-A removal using Raw and Biochar banana Peel adsorbents.

favorable thermodynamically. Furthermore, values of R^2 as obtained in the case of the treated sample (0.99) is higher than that for the raw peel (0.93), showing a stronger correlation and a better fit to the Langmuir model. This inferred that adsorption of BPA on treated peel is more consistent with monolayer coverage on a homogeneous surface.

Freundlich isotherm

The Freundlich isotherm is an empirical model that describes multilayer adsorption on heterogeneous surfaces. Mathematically, the linear representation of this model is shown in Eq. 10[37,40]:

$$InQ_e = InK_F + {}^{1}/_{n}C_e \tag{10}$$

Here, the constant of Freundlich is depicted as K_F (mg/g), while 1/*n* is the adsorption intensity constant.The data obtained from Fig. 9b are presented in Table 2. Using the linear regression method, the constant of Freundlich (K_F), that indicates adsorption capacity were found to be 66.12 (mg/g)(L/mg)$^{-1/n}$ and 45.51 (mg/g)(L/mg)$^{-1/n}$ for treated and raw peel respectively. The values of 1/n where deduced to be 0.27 and 0.50 for treated and raw peel with the treated peel sample having a lower value indicating stronger binding affinity than the raw peel. Furthermore, the R^2 values (0.97 for treated and 0.95 for raw) indicate good fit, though the treated sample fits better, implying a more heterogeneous adsorption surface.

Dubinin–Radushkevich

The Dubinin–Radushkevich (D–R) isotherm, is normally deploy to distinguish between physical and chemical adsorption and the linear representation of this model, that of the Polanyi potential, and the mean free energy are represented in Eqs. 11, 12 and 13 respectively[37,40]:

$$InQ_e = InQ_m - InK_{DR}^{\varepsilon^2} \tag{11}$$

$$\varepsilon = RTIn(1 + {}^{1}/_{C_e}) \tag{12}$$

$$E = 1/\sqrt{2K_{DR}} \tag{13}$$

The quantity of BPA adsorbed per unit mass of the adsorbent at equilibrium is given as Q_e, and is measured in mol/g. Whereas, Q_m denotes the maximum adsorption capacity representing the monolayer coverage, also expressed in mol/g. The mean adsorption energy, which is linked with the activity coefficient K_D, is given in units of mol^2/kJ^2. The Polanyi potential constant is represented by ε, R (8.3145 J·mol^{-1}·K^{-1}) denotes the ideal gas constant, while T stands for the absolute temperature in Kelvin. Using the linear regression method, the data obtained from Fig. 9c are presented in Table 2. The values of Q_s obtained are are 77.24 mg/g and 58.28 mg/g with the treated sample showing higher in aligning with other models depicting enhanced capacity. This was also corroborated from the R^2 values (0.94 and 0.97) for raw and treated samples respectively. The mean free energy (E) of adsorption for the raw banana peel was found to be 5.61 kJ/mol, which is an indication of physisorption[41]. On the contrary, the value of E for the treated peel was 16.19 kJ/mol, which falls within the range of chemisorption which is associated with stronger interactions involving the likes of ion exchange[41]. This trends supports previous findings from kinetic and confirms that the biochar treatment alters the nature of the interaction between BPA and the adsorbent surface. Pyrolysis at 600 °C eliminates a significant portion of volatile organic matter and hemicellulose, leading to increased porosity and surface area (as confirmed by BET results: raw = 84.21 m^2/g; biochar = 114.25 m^2/g). More importantly, pyrolysis alters the surface chemistry by concentrating aromatic carbon domains, exposing more oxygen-containing functional groups (e.g., phenolic –OH, carbonyl, and carboxyl), and causing some defect sites. FT-IR analysis show the disappearance of certain C–O peaks after adsorption, suggesting direct involvement of these groups in BPA binding. For the raw peel, adsorption is mainly governed by weaker forces such as van der Waals interactions and hydrogen bonding, consistent with the lower adsorption energy (E = 5.61 kJ/mol). After biochar treatment, the adsorption possesses much higher energy (E = 16.19 kJ/mol), indicative of chemisorption. This shift indicates stronger, more specific interactions between BPA and the biochar surface, like π–π electron donor–acceptor interactions between the

Adsorbents	BPA concentration	pH	Time	Dosage	Adsorption capacities (mg/g)	References
Activated carbon walnut shell (ACWS)	200 mg/L	2–5	100 min	0.09 g	115.85	[42]
Aliquat 336-impregnated magnetic multiwalled carbon nanotubes	10 mg/L	12	48 h	3 g	43.48	[43]
Activated *Tithonia diversifolia*	40 mg/L	7	80 min	0.2 g	15.69	[28]
commercial activated carbon (AC)	150 mg/L	2	120 min	60 mg	61.67	[44]
magnetic commercial activated carbon (MAC),	150 mg/L	2	120 min	60 mg	92.27	[44]
activated carbon from walnut shell (AW)	150 mg/L	2	120 min	60 mg	55.48	[44]
magnetic activated carbon from walnut shell (MAW)	150 mg/L	2	120 min	60 mg	89.23	[44]
Banana bunch	100 mg/L	3		100 mg	4.53	[24]
Coconut bunch	100 mg/L	3		100 mg	4.66	[24]
Empty fruit bunch activated carbon	20 mg/L	2–9	48 h	1 g	41.98	[37]
Activated carbon of Musa acuminata.	40 mg/L	5	3 h	9 mg	33.44	[33]
Activated carbon	50 mg/L	2		0.2 g	32.2	[45]
Raw banana peel	240 mg/L	8	200 min	0.4 g	91.3	This work
Treated banana peel	240 mg/L	8	150 min	0.4 g	135.2	This work

Table 3. Comparison of the adsorption capacities of Raw and treated banana Peel adsorbent for BPA uptake with others from literature.

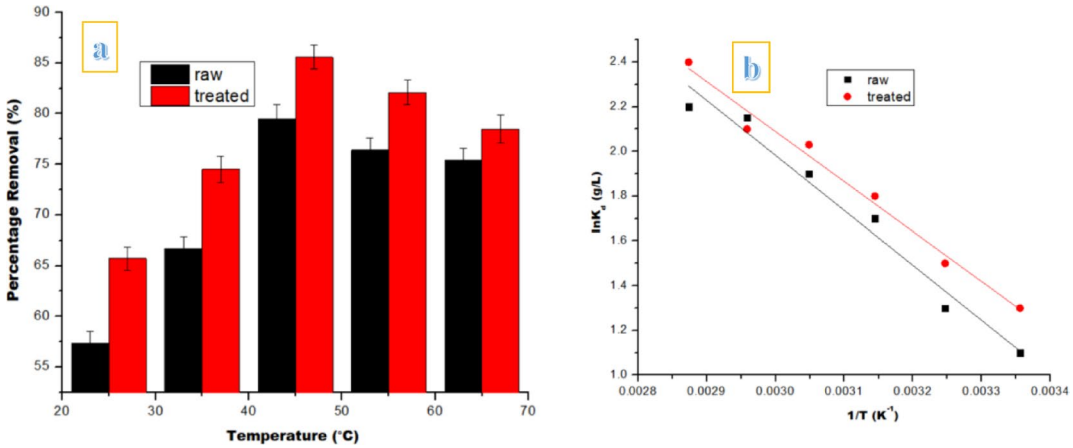

Fig. 10. Impact of temperature (a) and thermodynamic investigation of BPA adsorption by raw and treated banana peel.

condensed aromatic domains in biochar and the aromatic rings of BPA, as well as possible covalent or ion-exchange-like bonding with oxygenated functional groups.

Table 3 compares the maximum adsorption capacities (Q_{max}) of the raw and treated banana peel adsorbents obtained in this study with those of other reported low-cost and commercial materials for BPA elimination. The treated peel biochar exhibited a capacity of 135.2 mg/g, which is approximately 48% higher than that of the raw peel (91.3 mg/g) under identical experimental conditions. When compared to other biosorbents, the biochar from this study outperforms several agricultural waste-derived adsorbents. For instance, its capacity is more than 28 times greater than that of coconut bunch (4.66 mg/g) and banana bunch (4.53 mg/g) under similar pH conditions, and three times higher than the capacity reported for activated carbon obtained from *Musa acuminata* (33.44 mg/g)[33]. It also surpasses activated *Tithonia diversifolia* biomass (15.69 mg/g)[28] and oil palm empty fruit bunch activated carbon (41.98 mg/g)[37]. Even against some engineered carbon-based adsorbents, the treated biochar performs competitively; for instance, its Q_{max} is comparable to or exceeding certain commercial activated carbons such as ACWS (115.85 mg/g) and higher than magnetic activated carbon from walnut shell (89.23 mg/g)[42].

Effects of temperature and thermodynamic investigation

The role played by temperature on the sorption of BPA by raw and banana biochar reveals significant insights into understanding the adsorption mechanisms and the thermodynamics of these materials. The data provided by Fig. 10a reveals clearly that the sorption is temperature-dependent for both adsorbents across the tested range of temperature. Specifically, the adsorption percentage of BPA increases from 57.3% at 25 °C to a maximum of 79.5% at 45 °C for the raw banana adsorbent, and beyond 45 °C, the sorption starts to decline slightly, until reaching to 76.4% at 55 °C and 75.4% at 65 °C. The possible decline in adsorption efficiency beyond 45 °C? could be a combination of (i) weakened specific interactions (hydrogen bonding/π–π) due to rise in thermal

motion and (ii) increased aqueous-phase solubility and diffusivity of BPA that shifts the adsorption–desorption equilibrium slightly toward the solution phase at elevated temperatures. Likewise, for the biochar, adsorption efficiency shows an increasing trend as the temperature rose with adsorption efficiency rising from 65.7% at 25 °C to a peak of 85.6% at 45 °C. On attaining the peak of adsorption at 45 °C by biochar, it shows a slight reduction to 82.1% at 55 °C and 78.5% at 65 °C, which is similar to the behaviour observed with the raw banana peel. These minor reductions suggest that overly high temperatures may reduce the physical binding of dye molecules or alter the structure of the biochar surface, limiting dye attachment[41,42]. The rise in adsorption efficiency with temperature for both adsorbent is an indication of a positive temperature effect in this range as the trend indicates an endothermic process, with higher temperatures favoring dye uptake[44,46]. This is probably due to the enhanced mobility of the molecules of dye and the increase in their penetration ability into the adsorbent's pores.

In thermodynamic study, the parameters considered are the enthalpy change (ΔH), Gibbs free energy change (ΔG), and entropy change (ΔS), which together help to better explain the heat effects, feasibility, and randomness that is associated with the adsorption mechanism. Equation 14 to 16 were used to elucidate these parameters as provided below[41,44,46]:

$$K_d = {}^{q_e}/_{C_e} \tag{14}$$

$$\ln K_d = {}^{\Delta S^o}/_{R} - {}^{\Delta H^o}/_{RT} \tag{15}$$

$$\Delta G^o = RTInK_d \tag{16}$$

The data presented in Table 4 were obtained from Fig. 10b. Across the temperature range, the values of ΔG are negative for both raw and treated banana peels, suggesting spontaneous adsorption process[34,35,39]. It was noticed that the spontaneity is more pronounced in the case of the treated banana peel with values of − 5.84 kJ/mol for the raw peel and − 9.51 kJ/mol for the treated peel at 338 K. For the raw banana peel, the values of ΔH obtained is 17.42 kJ/mol, while for the treated peel, the value is much higher at 45.01 kJ/mol indicating endothermic process for both adsorbent[42]. The thermodynamic parameter of ΔH provides information about the adsorption mechanism, with values below 40 kJ/mol indicating physisorption, but when the values are above this threshold, it inferred chemisorption[47]. In this study, the ΔH values for BPA by raw and treated peel were found to be 17.42 kJ/mol and 45.01 kJ/mol, respectively, indicating that the raw peel adsorbent interacts with the BPA primarily through physisorption mechanisms, while the treated peel interacts via chemisorption mechanisms. The values of ΔS for both raw and treated banana peels are positive (8.62 J/mol·K and 16.26 J/mol·K) respectively which implies an increase in disorder or randomness at the solid–solution interface during the sorption process[42]. The greater ΔS value in the case of the treated banana peel indicates a more change in system disorder.

Desorption investigation

The study on desorption of BPA from raw banana and banana biochar helps to assess the efficiency and reusability of these adsorbents in multiple adsorption-desorption processes. As shown in Fig. 11, the desorption percentage for raw banana, begins at 73.2% in the first cycle and gradually declines to 70.2% in the second, 68.3% in the third, 63.2% in the fourth, and 58.9% in the fifth cycle. On the other hand, banana biochar shows better desorption behavious throughout with the desorption efficiency starting from 79.3% in the first cycle and then shows a slower reduction to 77.5%, 75.6%, 69.4%, and 66.7% in the second to fifth cycles respectively. The gradual decline suggests partial loss or structural degradation, saturation of active sites, or possibly strong irreversible interactions between the banana surface and the dye molecules. The biochar was observed to have outperforms raw banana, and this could be attributed to improved higher surface area, porosity and most likely, better thermal stability of biochar. These properties permit easy release of dye molecules, and the structure of the biochar becomes more stable thus preventing the deterioration of its adsorption-desorption capacity when subjected to repeated use. Though both adsorbents experience a decline in desorption efficiency over multiple cycles, their rate of decline is relatively small with the biochar and the raw still maintaining over 66% and 60% desorption even after five operational cycles.This suggests that banana peel biochar is a low-cost, effective, and sustainable adsorbent for BPA removal.

	Raw			Treated		
T (K)	ΔG (kJ/mol)	ΔH (kJ/mol)	ΔS (J/mol·K)	ΔG (kJ/mol)	ΔH (kJ/mol)	ΔS (J/mol·K)
298	−1.11			−3.63		
308	−2.77			−5.84		
318	−3.68			−6.56		
328	−4.88	17.42	8.62	−8.85	45.01	16.26
338	−5.84			−9.51		

Table 4. Thermodynamics variables of the adsorption of bisphenol-A by Raw and Biochar banana peel.

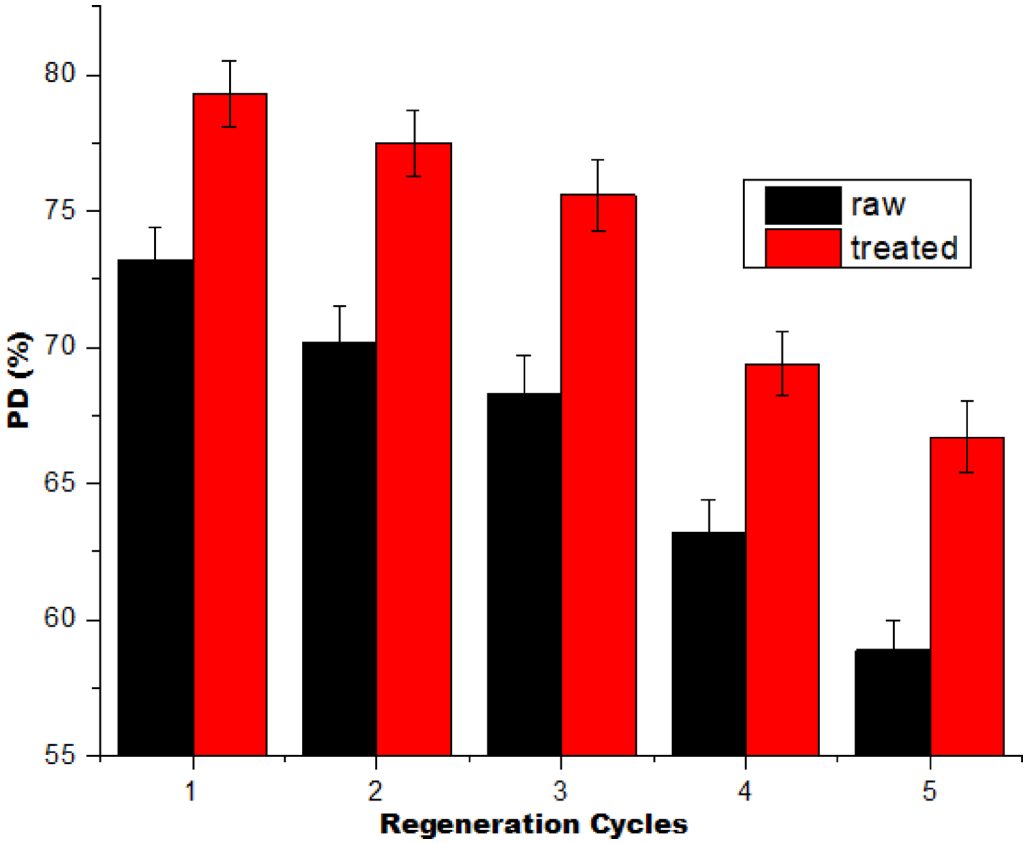

Fig. 11. Desorption of BPA using 0.1 M EDTA for raw and treated banana peel.

Interference of co-contaminants with BPA adsorption

Wastewater streams containing Bisphenol-A may also contained other organic and inorganic pollutants, which can compete for active sites on adsorbent surfaces, altering surface charge, or change the chemical environment, which could affect the removal efficiency of BPA. In the current analysis, common potential co-contaminants like di-n-butyl phthalate (DBP), di(2-ethylhexyl) phthalate (DEHP), chloride (Cl^-), arsenic (As), malachite green (MG), lead (Pb^{2+}), cadmium (Cd^{2+}), and Congo red (CR) were examined as shown in Fig. 12.

The results reveal that BPA removal (70.2%) was markedly higher than for other contaminants, suggesting a preferential affinity of the banana peel biochar toward aromatic endocrine disruptors with phenolic groups. DBP (45.4%) and MG (40.3%) also showed moderate removal, which may be due to similar hydrophobic and π–π interaction mechanisms with the biochar's carbonaceous surface. Heavy metals such as Cd^{2+} and Pb^{2+} also exhibited intermediate removal (39–45%), probably through complexation with oxygen-containing functional groups; however, their presence could partially block active sites and reduce BPA uptake if concentrations are high.

Inorganic anions like Cl^- and metalloid contaminants such as As showed lower removal (< 22%), reflecting weaker electrostatic or complexation interactions with the adsorbent under the tested conditions. CR and DEHP had the lowest removal (10–12%), likely due to low affinity for the active sites or steric hindrance. This variation in removal efficiency underscores the possibility of competitive adsorption in real wastewater systems, where multiple organic and inorganic pollutants coexist. Such competition may reduce BPA sorption, particularly when co-contaminants share similar binding mechanisms (e.g., hydrophobic interactions or π–π stacking).

Estimated adsorbent cost

Table 5 presents the estimated cost of production per kilogram of the raw and treated adsorbents. For instance, the cost of the raw sample are solely from drying and grinding ($0.15/kg) and labor/miscellaneous expenses ($0.10–$0.18/kg), giving a total cost of $0.25–$0.33/kg. In contrast, the treated sample incurs additional pyrolysis energy costs of $0.0708–$0.1667/kg, which elevates the total estimated cost to $0.3208–$0.4967/kg. The absence of a cost for raw material in both cases indicates its origin as an agricultural waste, making both adsorbents highly economical compared to adsorbents that require purchased feedstocks. However, the treated sample's higher cost is justified by its improved adsorption performance, which is often observed due to enhanced surface area, porosity, and functional group activation during pyrolysis which eventually enhanced its adsorption performance. When compared with the price of commercial activated carbon, the stark difference underlines the economic advantage of using agricultural waste-derived adsorbents which remains far less expensive while still providing competitive adsorption capacity for pollutant removal.

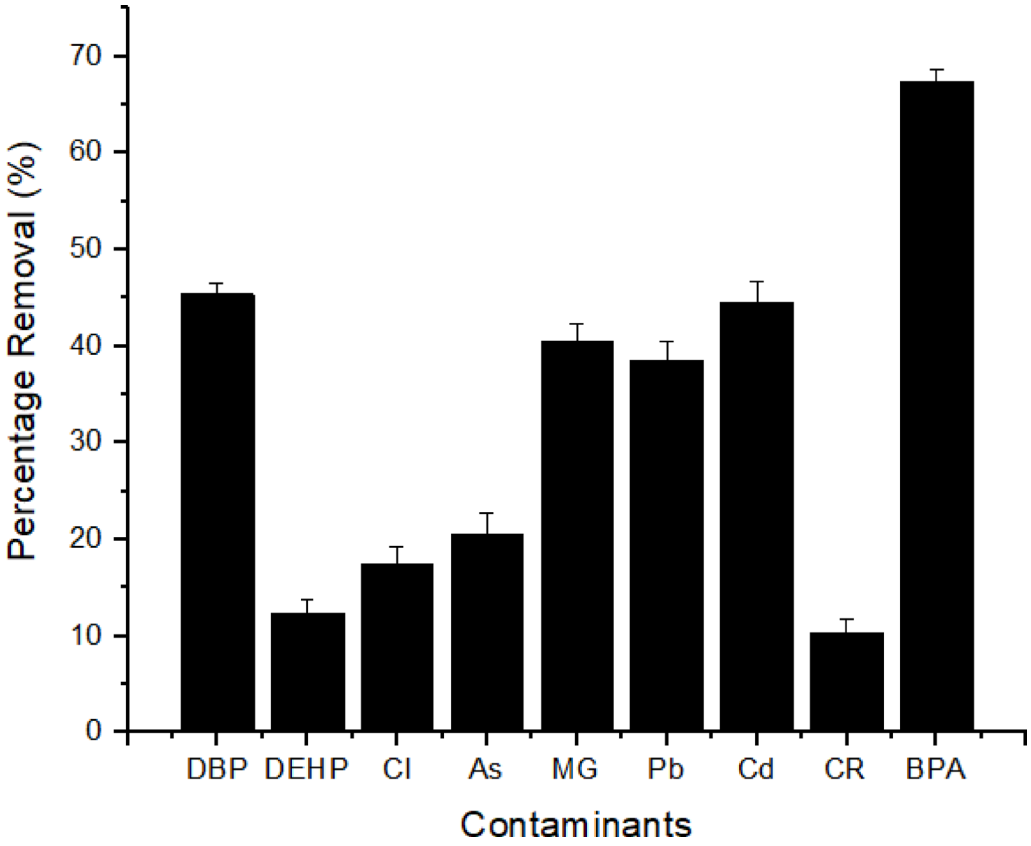

Fig. 12. Effect of co-contaminants with BPA.

Cost Component	Estimated Cost (USD/kg) for raw sample	Estimated Cost (USD/kg) for treated sample
Raw material	0.00	0.00
Drying and grinding	$0.15	$ 0.15
Pyrolysis (energy only)	nil	$0.0708 –$0.1667
Labor + Miscellanous	$0.10–0.18	$0.10–0.18
Total Estimated Cost	$0.25–$0.33	$0.3208–0.4967

Table 5. Estimated cost of adsorbent per 1 kg.

Conclusions

This study evaluated the performance of raw banana peel and banana peel biochar for the elimination of bisphenol-A (BPA) from aqueous solutions under varying experimental conditions. Pore structure analysis showed that both adsorbents were predominantly mesoporous, with pore sizes ranging from 1.8 to 2.8 nm and pore volume distribution concentrated between 2.4 and 2.8 nm. SEM observations suggested notable morphological changes after BPA adsorption, with declined surface porosity confirming the attachment of BPA molecules to the adsorbent matrix. Maximum uptake was achieved at 150 min for the raw sample and 200 min for the biochar at an initial BPA concentration of 240 mg/L. The adsorption mechanism for the biochar was consistent with chemisorption, while that of the raw material was governed by physisorption. Thermodynamic analysis confirmed that the process was spontaneous and endothermic. Overall, banana peel biochar exhibited enhanced BPA removal efficiency compared to raw banana peel, highlighting its potential as a cost-effective and sustainable adsorbent. However, future work could involved column and/or pilot scale experiments to validate the adsorbent's performance under practical operating conditions.

Data availability

The datasets used and/or analysed during the current study available from the corresponding author on reasonable request.

Received: 18 July 2025; Accepted: 25 August 2025
Published online: 27 August 2025

References

1. Tappert, L. et al. Bisphenol A in surface waters in germany: part I. Reassessment of sources and emissions pathways for FlowEQ modeling. *Integr. Environ. Assess. Manag.* **20**, 21–125. https://doi.org/10.1002/ieam.4805 (2023).
2. Almeida, S., Raposo, A., Almeida-Gonzalez, M. & Carrascosa, C. Bisphenol A: food exposure and impact on human health. *Compr. Rev. Food Sci. Food Saf.* https://doi.org/10.1111/1541-4337.12388 (2018).
3. Czarny-Krzymińska, K., Krawczyk, B. & Szczukocki, D. Bisphenol A and its substitutes in the aquatic environment: occurrence and toxicity assessment. *Chemosphere* **315**, 137763. https://doi.org/10.1016/j.chemosphere.2023.137763 (2023).
4. Inadera, H. Neurological effects of bisphenol A and its analogues. *Int. J. Med. Sci.* **12**, 926–936. https://doi.org/10.7150/ijms.13267 (2015).
5. Semerjian, L., Alawadhi, N. & Nazer, K. Detection of bisphenol A in thermal paper receipts and assessment of human exposure: a case study from Sharjah. *United Arab. Emirates*. https://doi.org/10.1371/journal.pone.0283675 (2023). PloSOne.
6. Yu, C. et al. Development of a novel biochar/iron oxide composite from green algae for bisphenol-A removal: adsorption and Fenton-like reaction. *Environ. Technol. Innov.* https://doi.org/10.1016/j.eti.2022.102647 (2022).
7. Zhu, H., Li, Z. & Yang, J. A novel composite hydrogel for adsorption and photocatalytic degradation of bisphenol A by visible light irradiation. *Chem. Eng. J.* https://doi.org/10.1016/j.cej.2017.11.148 (2018).
8. Tokula, B. E., Dada, A. O., Inyinbor, A. A., Obayomi, K. S. & Olugbenga Solomon Bello and Ujjwal Pal. Agro-waste based adsorbents as sustainable materials for effective adsorption of bisphenol A from the environment: A review. *J. Clean. Prod.* https://doi.org/10.1016/j.jclepro.2022.135819 (2023).
9. Mojiri, A. Treatment of water and wastewater: challenges and solutions. *Separations* **10**(7), 385. https://doi.org/10.3390/separations10070385 (2023).
10. Ofudje, E. A., Adeogun, A. I., Idowu, M. A., Kareem, S. O. & Ndukwe, N. A. Simultaneous removals of cadmium(II) ions and reactive yellow 4 dye from aqueous solution by bone meal-derived apatite: kinetics, equilibrium, and thermodynamic evaluations. *J. Anal. Sci. Technol.* **11** https://doi.org/10.1186/s40543-020-0206-0 (2020).
11. Adegoke, K. A. et al. Modified biomass adsorbents for removal of organic pollutants: A review of batch and optimization studies. *Int. J. Environ. Sci. Technol.* https://doi.org/10.1007/s13762-023-04872-2 (2023).
12. Kaci, M. M., Akkari, I., Pazos, M., Atmani, F. & Akkari, H. Recent trends in remediating basic red 46 dye as a persistent pollutant from water bodies using promising adsorbents: a review. *Clean. Techn Environ. Policy*. **27**, 773–788. https://doi.org/10.1007/s10098-024-03026-3 (2025).
13. Tiliouine, Y. et al. Powdered Myrtle leaves: A sustainable biosorbent for effective methylene blue adsorption. *Water Conserv. Sci. Eng.* **9**, 31. https://doi.org/10.1007/s41101-024-00265-9 (2024).
14. Akkari, I., Kaci, M. M. & Pazos, M. Revolutionizing waste: Harnessing agro-food hydrochar for potent adsorption of organic and inorganic contaminants in water. *Environ. Monit. Assess.* **196**, 1035. https://doi.org/10.1007/s10661-024-13171-3 (2024).
15. Kasambala Hildegard, R., Mwemezi, J. & Rwiza Nelson mpumi, Mwema Felix Mwema & Karoli K. Njau. (2025). Biochars derived from banana and Mango peels in isolated systems revealed high removal efficiency of endocrine-disrupting compounds from water. *Biomass Conv Bioref.* **15**, 13575–13588. https://doi.org/10.1007/s13399-024-06196-8 (2025).
16. Hussin, F., Aroua, M. K. & Szlachta, M. Biochar derived from fruit by-products using pyrolysis process for the elimination of Pb (II) ion: an updated review. *Chemosphere* **287**, 132250. https://doi.org/10.1016/j.chemosphere.2021.132250 (2022).
17. Farias, K. C. S. et al. Banana Peel powder biosorbent for removal of hazardous organic pollutants from wastewater. *Toxics* **11** (8), 664. https://doi.org/10.3390/toxics11080664 (2023).
18. Akpomie, K. G. & Conradie, J. Banana Peel as a biosorbent for the decontamination of water pollutants. A review. *Environ. Chem. Lett.* **18**, 1085–1112. https://doi.org/10.1007/s10311-020-00995-x (2020).
19. Sánchez Orozco, R. et al. C. E., and Characterization of lignocellulosic fruit waste as an alternative feedstock for bioethanol production, biores. 1873–1885. (2014). https://doi.org/10.15376/biores.9.2.1873-1885
20. Munagapati, V. S. et al. Adsorptive removal of anionic dye (Reactive black 5) from aqueous solution using chemically modifed banana Peel powder: kinetic, isotherm, thermodynamic, and reusability studies. *Int. J. Phytorem.* **22**, 267–278. https://doi.org/10.1080/15226514.2019.1658709 (2020).
21. Mondal, N. K. & Kar, S. Potentiality of banana Peel for removal of congo red dye from aqueous solution: isotherm, kinetics and thermodynamics studies. *Appl. Water Sci.* **8**, 157. https://doi.org/10.1007/s13201-018-0811-x (2018).
22. Yang, X. et al. Surface functional groups of carbon-based adsorbents and their roles in the removal of heavy metals from aqueous solutions: a critical review. *Chem. Eng. J.* **366**, 608–621. https://doi.org/10.1016/j.cej.2019.02.119 (2019).
23. Alghamdi, A. A. et al. Efficient adsorption of lead (II) from aqueous phase solutions using polypyrrole-based activated carbon. *Materials* **12** https://doi.org/10.3390/ma12122020 (2019).
24. Mat, L. Z. et al. Bisphenol a removal by adsorption using waste biomass: isotherm and kinetic studies. *Biointerface Res. Appl. Chem.* **11** (1), 8467–8481 (2021).
25. Shenwari1, K. A., Priyatharshini, S., Dhevagi, P., Chitdeshwari, T. & Avudainayagam, S. Removal of lead and cadmium from aqueous solutions by banana Peel Biochar. *Madras Agric. J.* **106** (1–3), 45–53. https://doi.org/10.29321/MAJ2019.000220 (2019).
26. Urgel, J. J. D. T. et al. Removal of diesel oil from water using Biochar derived from waste banana peels as adsorbent. *Carbon Res.* **3**, 13. https://doi.org/10.1007/s44246-024-00100-9 (2024).
27. Wang, J. & Zhang, M. Adsorption characteristics and mechanism of bisphenol A by magnetic Biochar. *Int. J. Environ. Res. Public Health*. **17** (3), 1075. https://doi.org/10.3390/ijerph17031075 (2020).
28. Supong, A. et al. Adsorptive removal of bisphenol A by biomass activated carbon and insights into the adsorption mechanism through density functional theory calculations. *Sustainable Chem. Pharm.* **13**, 100159. https://doi.org/10.1016/j.scp.2019.100159 (2019).
29. Chen, Y., Jingci, J. T. H. S., Liu, H., Wang, F. & Sun, L. Development of a novel biochar/iron oxide composite from green algae for bisphenol-A removal: adsorption and Fenton-like reaction. *Environ. Technol. Innov.* **28**, 102647. https://doi.org/10.1016/j.eti.2022.102647 (2022).
30. Kumar, S. A. P., Nagarajan, R., Anand, B. & Prasad.K. M., and Thermogravimetric study and kinetics of banana Peel pyrolysis: a comparison of 'model-free' methods. *Biofuels* **13** (2), 1–10. https://doi.org/10.1080/17597269.2019.1647375 (2019).
31. Lopez, H. D., Ayala, N. & Malagón-Romero, D. Evaluation of the production of bio-oil obtained through pyrolysis of banana Peel waste. *Chem. Eng. Trans.* **89**, 637–642. https://doi.org/10.3303/CET2189107 (2021).
32. Ounis, M. et al. Optimisation of adsorption removal of bisphenol A using Sludge-Based activated carbons: application of response surface methodology with a Box–Behnken design. *Arab. J. Sci. Eng.* **49**, 497–514. https://doi.org/10.1007/s13369-023-08203-y (2024).
33. Rahmat, N. A., Hadibarata, T., Yuniarto, A., Elshikh, M. S. & Syafiuddin, A. Isotherm and kinetics studies for the adsorption of bisphenol A from aqueous solution by activated carbon of Musa acuminata. *IOP Conf. Series: Mater. Sci. Eng.* **495** (1), Article012059. https://doi.org/10.1088/1757-899X/495/1/012059 (2019).
34. Sirach, R. & Dave, P. N. Thermal and bisphenol-A adsorption properties of a zinc ferrite/β-cyclodextrin polymer nanocomposite. *RSC Adv.* **13**, 21991–22006. 10.1039/D3RA03331G. (2023).
35. Uddin, M., Venkatesan, S. K., Sekar, K., Ramasamy, B. & Kandasamy, R. T. Interfacial interaction mechanisms of ameliorated Surface-Active/π-Electron-Rich designer bioamphiphile via Environmental-Waste Bio-upcycling for trace bisphenol A removal from municipal landfill leachate. *ACS Sustainable Resour. Manage.* **1** (9), 1962–1974. https://doi.org/10.1021/acssusresmgt.4c00087 (2024).

36. Matharage, H. et al. From waste to resource: King coconut Biochar as a green adsorbent for bisphenol A removal. *Case Stud. Chem. Environ. Eng.* **12**, 101261. https://doi.org/10.1016/j.cscee.2025.101261 (2025).
37. Ahmed, M. B., Zhou, J. L., Ngo, H. H., Johir, M. A. & Sornalingam, K. Sorptive removal of phenolic endocrine disruptors by functionalized biochar: competitive interaction mechanism, removal efficacy and application in wastewater. *Chem. Eng. J.* **335**, 801–811 (2018).
38. Wirasnita, R., Hadibarata, T., Yusoff, A. R. M. & Yusop, Z. Removal of bisphenol A from aqueous solution by activated carbon derived from oil palm empty fruit bunch. *Water Air Soil. Pollut.* **225**, 2148. https://doi.org/10.1007/s11270-014-2148-x (2014).
39. Shao, Z., Wu, S., Gao, Y., Liu, X. & Dai, Y. Two-step pyrolytic Preparation of Biochar for the adsorption study of Tetracycline in water. *Environ. Res.* **242**, 117566. https://doi.org/10.1016/j.envres.2023.117566 (2024).
40. Al-sareji, O. J. et al. A sustainable banana Peel activated carbon for removing pharmaceutical pollutants from different waters: production, characterization, and application. *Materials* **17**, 1032. https://doi.org/10.3390/ma17051032 (2024).
41. El-Rayyes, A. et al. L. A., and Hot water-treated cow waste use as an efficient adsorbent for cresol red dye and chromium VI removal from aqueous solutions, *BioResources* **20** (2), 3252–3285. (2025). https://doi.org/10.15376/biores.20.2.3252-3285
42. Uzosike, A. O. et al. Magnetic supported activated carbon obtained from walnut shells for bisphenola uptake from aqueous solution. *Appl. Water Sci.* **12**, 201. https://doi.org/10.1007/s13201-022-01724-1 (2022b).
43. Bhatia, D. & Datta, D. Removal of bisphenol-a using amine-modifed magnetic multiwalled carbon nanotubes: batch and column studies. *J. Chem. Eng. Data*. **64**, 2877–2887 (2019).
44. Uzosike, A. O., Ofudje, E. A., Adeogun, A. I., Akinyele, J. O. & Idowu, M. A. Comparative analysis of bisphenol-A removal efficiency from water: equilibrium, kinetics, thermodynamics and optimization evaluations. *J. Iran. Chem. Soc.* **19**, 4645–4658. https://doi.org/10.1007/s13738-022-02628-2 (2022).
45. Mourao, P. et al. Adsorption of bisphenol A by granular activated carbon prepared with diferent silicates as binders. *Int. J. Environ. Sci. Technol.* **21**, 3719–3734 (2024).
46. Ofudje, E. A., Al-Ahmary, K. M. & Alzahrani, E. A. Sugarcane Peel Ash as a sorbent for methylene blue. *BioResources* **19** (4), 9191–9219. https://doi.org/10.15376/biores.19.4.9191-9219 (2024).
47. Mchich, Z. et al. Eco-friendly engineering of micro composite-based hydroxyapatite bio crystal and polyaniline for high removal of OG dye from wastewater: adsorption mechanism and RSM@BBD optimization. *Environ. Res.* **257**, 119289. https://doi.org/10.1016/j.envres.2024.119289 (2024).

Acknowledgements

The authors express their gratitude to Princess Nourah bint Abdulrahman University Researchers Supporting Project number (PNURSP2025R581), Princess Nourah bint Abdulrahman University, Riyadh, Saudi Arabia.

Author contributions

Salah Ud Din carried out the characterizations and statistical analysis, Patrick T. Ngueagn performed the experiments and wrote the first draft, Khairia Mohammed Al-Ahmary read the first draft, and performed statistical analysis Hamad AlMohamadi performed data analysis and performed experiments Saedah R. Al-Mhyawi contributed materials resources and performed statistical analysis, Nuha Y. Elamin and Ibtehaj F. Alshdoukhi contributed materials resources, contributed in characterization and performed data analysis, Jawaher Saud Alrashood provided financial assistance and contributed resources, and Edwin A. Ofudje conceived the work, carried out the statistical analysis, and characterizations.

Funding

This work was funded by Princess Nourah bint Abdulrahman University Researchers Supporting Project number (PNURSP2025R581), Riyadh, Saudi Arabia.

Declarations

Competing interests

The authors declare no competing interests.

Additional information

Correspondence and requests for materials should be addressed to P.T.N.

Reprints and permissions information is available at www.nature.com/reprints.

Publisher's note Springer Nature remains neutral with regard to jurisdictional claims in published maps and institutional affiliations.